Histol Histopathol (2009) 24: 49-60

http://www.hh.um.es

Histology and Histopathology

Cellular and Molecular Biology

An innovative methodology for the automated morphometric and quantitative estimation of liver steatosis

Giuseppa Esterina Liquori[1], Giuseppe Calamita[2], Davide Cascella[3], Maria Mastrodonato[1], Piero Portincasa[4] and Domenico Ferri[1]

[1]Department of Zoology, Laboratory of Histology and Comparative Anatomy, University of Bari, Bari, Italy, [2]Department of General and Environmental Physiology, University of Bari, Bari, Italy, [3]Department of Electrotechnics and Electronics, Politecnico of Bari, Bari, Italy and [4]Department of Internal and Public Medicine, Section of Internal Medicine, University of Bari, Bari, Italy

Summary. The management of liver steatosis, due to its potential evolution towards severe diseases, requires accurate diagnosis. Fatty infiltration in liver diseases is commonly assessed histologically by semi-quantitative methods, which can be subjective. Automated computerized procedures using commercial software for image analysis have also been recently employed. The aim of the study was to develop an innovative automated computerized procedure to accurately evaluate both the morphometry and degree of lipid accumulation in liver. Fatty infiltration was assessed in paraffin- and resin-embedded samples of steatotic livers from rats undergoing 0, 3, 7, 14, and 30-day choline-deficient diet, and from liver biopsy of a morbidly obese patient undergoing bariatric surgery. Specific software was developed, which works with a morphological operator, in addition to a chromatic one to select lipid droplets. The choline-deficient diet induced steatosis with a gradual shift from micro- to macro-vesicular. In paraffin sections, the macrovesicles-to-microvesicles ratio and the degree of steatosis, when using only the chromatic operator, produced overestimates. Results were consistent in both rat and human samples. An improvement of topographic, morphometric and quantitative estimation of fatty liver infiltration is obtained with our software, working with a morphological operator and using semi-thin sections from resin-embedded samples. This innovative procedure may be applied to human liver samples, offering promising diagnostic and prognostic perspectives.

Offprint requests to: Prof. Domenico Ferri, Dipartimento di Zoologia, Laboratorio di Istologia e Anatomia comparata, Via Orabona, 4 I-70125 Bari, Italy. e-mail: d.ferri@biologia.uniba.it

Key words: Liver steatosis, Steatohepatitis, Image analysis, Choline deficient diet, Microscopy

Introduction

Liver steatosis comprises abnormal accumulation of triglycerides in hepatocytes in response to metabolic, toxic, and viral conditions (Portincasa et al., 2006; Calamita and Portincasa, 2007). The most frequent form, namely the non-alcoholic fatty liver disease (NAFLD) was firstly described as a form of chronic liver disease, resembling the histological changes of alcoholic liver disease but found in subjects who do not abuse alcohol (Ludwig et al., 1980). Patients, instead, are often carriers of metabolic conditions, such as insulin resistance or diabetes, overweight, obesity, and dyslipidemia and are not affected by autoimmune, viral, neoplastic or rarer liver diseases. Histology of NAFLD, however, is indistinguishable from that of alcoholic hepatitis (Ludwig et al., 1980). The fatty liver is typically discovered in the clinical setting during routine abdominal ultrasonography, showing a "bright liver". From an epidemiological point of view, NAFLD can be considered an example of a “mass disease”, with a prevalence ranging between 20 and 40% in the adult population in Western countries (Neuschwander-Tetri and Bacon, 1996; Loguercio et al., 2001, 2004). The prevalence of NAFLD is growing worldwide due to the increasing prevalence of obesity, diabetes and the metabolic syndrome. This latter condition is a constellation of variables associated with insulin resistance that puts subjects at high risk for cardiovascular morbidity and mortality (Marchesini et al., 2003; Loguercio et al., 2004; Kahn et al., 2005). NAFLD is currently deemed as the most common cause

of chronic liver disease in humans (Portincasa et al., 2005) with potential harmful evolution towards the necro-inflammatory form of non-alcoholic steato-hepatitis (NASH) in 10-15% of the cases (Matteoni et al., 1999) and liver cirrhosis in 20% of NASH patients, and a cumulative payload associated with NAFLD estimated to account for 30-40% of all deaths from liver diseases (Poonawala et al., 2000). Although imaging techniques, including hepatic ultrasonography, computed tomography and nuclear magnetic resonance have high sensitivity and specificity (>90%) for the diagnosis of liver steatosis itself, the ultimate diagnosis of NAFLD/NASH requires invasive liver biopsy, followed by histology, to quantify the true degree of steatosis, fibrosis and necroinflammatory changes (Brunt et al., 1999). Morphologically, liver steatosis is classified as either macrovesicular or microvesicular in type (Burt et al., 1998; Fong et al., 2000). Microvesicular steatosis is characterised by the presence within the hepatocytes of numerous small lipid vesicles, having a mean diameter of less than 15 μm (Zaitoun et al., 2001), or less than the mean diameter of the hepatocyte nucleus (Marsman et al., 2004). In contrast, macrovesicular steatosis is characterised by the presence of a large fat globule that displaces the nucleus within hepatocytes. Microvesicular steatosis is generally a more severe disease than macrovesicular, and occurs in a variety of conditions with defective fatty acid ß-oxidation (Burt et al., 1998; Reddy an Mannaerts, 1994; Sherlock, 1995). Macrovesicular steatosis is generally deemed as a benign condition, being associated with changes to the lipid metabolism, and potentially reversible in most instances. Depending on liver diseases, fat globules may be restricted to centrilobular or periportal hepatocytes, or widely diffused throughout the hepatic lobule (panlobular steatosis). A correct histological typing and evaluation of the degree of steatosis are obviously important for both prognostic and diagnostic purposes. The determination of micro- and macrovesicular steatosis in donor livers is also crucial within the liver transplantation program (Urena et al., 1998). Fatty liver infiltration is commonly assessed by optical semiquantitative methods (Nagore and Scheuer, 1988). However, methods are inaccurate and can be highly subjective; computerized procedures using commercially available automated analysis softwares have also been tested on human liver biopsy specimens (Auger et al., 1986; Zaitoun et al., 2001; Marsman et al., 2004) and on rat models of liver steatosis obtained by choline-deficient diet (Marsman et al., 2004). In all cases, image analyses were performed on haematoxylin and eosin (H&E)-stained slides prepared from liver samples embedded in paraffin wax. The aims of this study were to (i) innovate an automated computerized methodology to assess the morphological and quantitative profile of fat liver accumulation, and (ii) provide novel insights into the clinico-pathological estimation of human liver steatosis. Automated analysis was set up with fatty livers obtained from rats undergoing a choline-deficient diet, and applied also to liver samples from a morbidly obese subject undergoing bariatric surgery.

Materials and methods

Adult male Wistar rats (weighting 250-350g; Harlan, S. Pietro al Natisone, Italy) were maintained on a standard diet and water *ad libitum*, kept in individual cages under controlled conditions of temperature and humidity and a constant 12-hour light/dark cycle, according to the Guide for the Care and Use of Laboratory Animals (National Institutes of Health). Animals had access to standard rat chow and tap water for the whole study period. Induction of fatty liver in the absence of necro-inflamatory and body weight changes was obtained by feeding rats with the choline-deficient diet (Dyets Inc., Bethlem, PA), as previously published by our group (Grattagliano et al., 2000, 2003) and others (Kulinski et al., 2004). This diet increases liver triglyceride content in the rodent model (Raubenheimer et al., 2006). The control group consisted of rats fed adequate levels of choline. Three rats from each group (i.e. choline-deficient diet and control diet) were killed after 0, 3, 7, 14 and 30 days of diet. Animals were anesthetized and their livers quickly removed. The study was approved by the State Committee on animal experimentation.

Human liver sections were obtained from the liver biopsy of a morbidly obese patient undergoing bariatric surgery after obtaining informed written consent. The procedure was part of a routine histological examination of a macroscopically-evident fatty liver.

Histological studies

Either rat or human liver samples were fixed in 10% formalin solution and processed for paraffin-wax embedding. Other samples were fixed in 4% glutaraldehyde and processed for embedding in Epoxy Resin-Araldite (M) CY212 (TAAB, Aldermaston, England). Sections (5 μm thick) from paraffin-embedded specimens were routinely stained with haematoxylin-eosin (H&E) and with periodic acid-Schiff (PAS). Semi-thin sections (2 μm thick) from epoxy resin embedded specimens, obtained using a Ultratome III ultramicrotome (LKB, Bromma, Sweden), were sequentially stained with Toluidine blue-PAS (PAS-TB). For quantitative histological analyses, at least 6 digital pictures (original magnification: 400x) were taken for each sample using a Nikon Eclipse 600 photomicroscope equipped with a Nikon DMX 1200 camera (Nikon Instruments SpA, Calenzano, FI, Italy).

Image analysis

The image analysis software was developed with the MathWorks Matlab 2007b. Histologically, lipid droplets are characterised by chromatic uniformity and circular shape. These features were used as discrimination

criteria in developing algorithms for the automated image-processing software. The software operates the following three algorithms: image conditioning (data pre-processing), chromatic and morphologic analysis (pattern recognition), and classification and output generation (interpreting results). Image conditioning is necessary to correct the spatial chromatic gradients which typically occur when the image is captured with non-uniform lighting. To select the lipid areas, chromatic and morphological analysis follows four steps (Fig. 1). Starting from an initial chromatic reference (algorithm initialization), the algorithm selects a blob mask (set of segmented regions) containing all the lipids but also false positive cases. As a second step, the blob mask is processed by an erosion filter (Haralick and Shapiro, 1992). This morphological operator reduces all the selected blobs and consequently discards any very small blobs caused by the chromatic noise in the image background. In the third step, a dilation filter extends the blobs to their original size (van den Boomgard and Van Balen, 1992). In the fourth step, the eccentricity filter further reduces the number of selected blobs by checking their shape (Matlab 2007b, The MathWorks, Natick, MA US). A statistical analysis, carried out on a sample of 500 lipid droplets, revealed that in 95% of cases their eccentricity index was less than 0.1. Hence, blobs with an eccentricity index greater than 0.1 are excluded. False positive cases are discarded, e.g. a sinusoid with the same colour and size as the lipids may pass the first three steps, but not the fourth because of their shape (far from a circle). Finally, the sets of blobs corresponding to lipids are finally divided into microvesicles, with a mean diameter of less than 15 µm, and macrovesicles with a mean diameter equal or larger than 15 µm, according to Zaitoun and co-workers (Zaitoun et al., 2001). Finally, the software generates the output report containing all relevant data.

Statistical analysis

Data are reported as means±standard error (SEM). For each experimental condition, data obtained from paraffin embedded specimens were compared to those obtained from resin embedded samples by the Student's *t*-test. A two-tailed *P* value of less than 0.05 was considered significant. All calculations were performed with the NCSS2007 statistical software (Kaysville, UT, USA) (Armitage and Berry, 1994; Dawson and Trapp, 2001).

Results

The appearance of normal and steatotic rat liver is depicted in Figure 2 (a,b) as gross examination. Histologically, in normal liver, cells exhibited significant heterogeneity within the hepatic lobule. Centrilobular hepatocytes were larger than those visible in the periportal area, while periportal hepatocytes showed a more extensive metachromatic cytoplasm, indicating a well developed rough endoplasmic reticulum (Fig. 2e,f). The PAS reaction showed that glycogen was dispersed in centrilobular hepatocytes, whereas it occupied large cytoplasmic areas in periportal hepatocytes (Fig. 2e,f). Lipid droplets were rare, accounting for 1.2±0.2% and 1.4 ± 0.3% in paraffin- and in resin-embedded sections, respectively (Fig. 2d,f), and mainly occurring in periportal hepatocytes. At gross examination, the steatotic liver in the animals fed the choline-deficient diet was yellowish and showed a time-dependent increase in size (Fig. 2b). Considerable fat accumulation was seen in the hepatocytes of rats at day 3 of the choline-deficient diet, whereas no increase in fat content

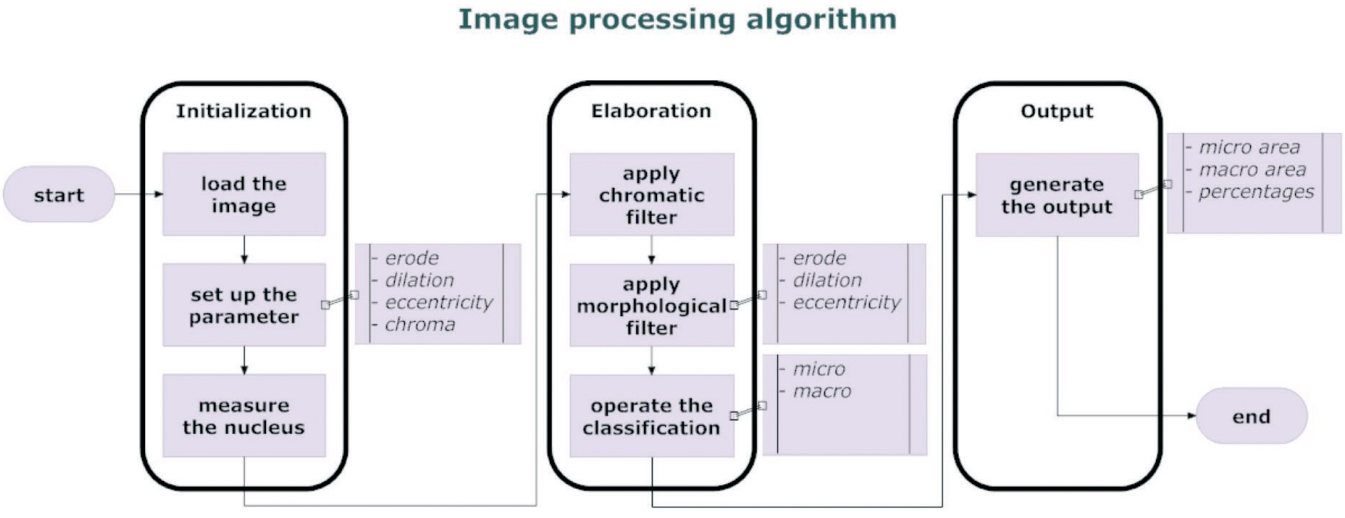

Fig. 1. Image processing algorithm used for the morphometric and quantitative evaluation of liver steatosis. Flow chart shows the execution steps that generate the outputs. The steps are collected in the three macro-blocks: initialization, elaboration, and output.

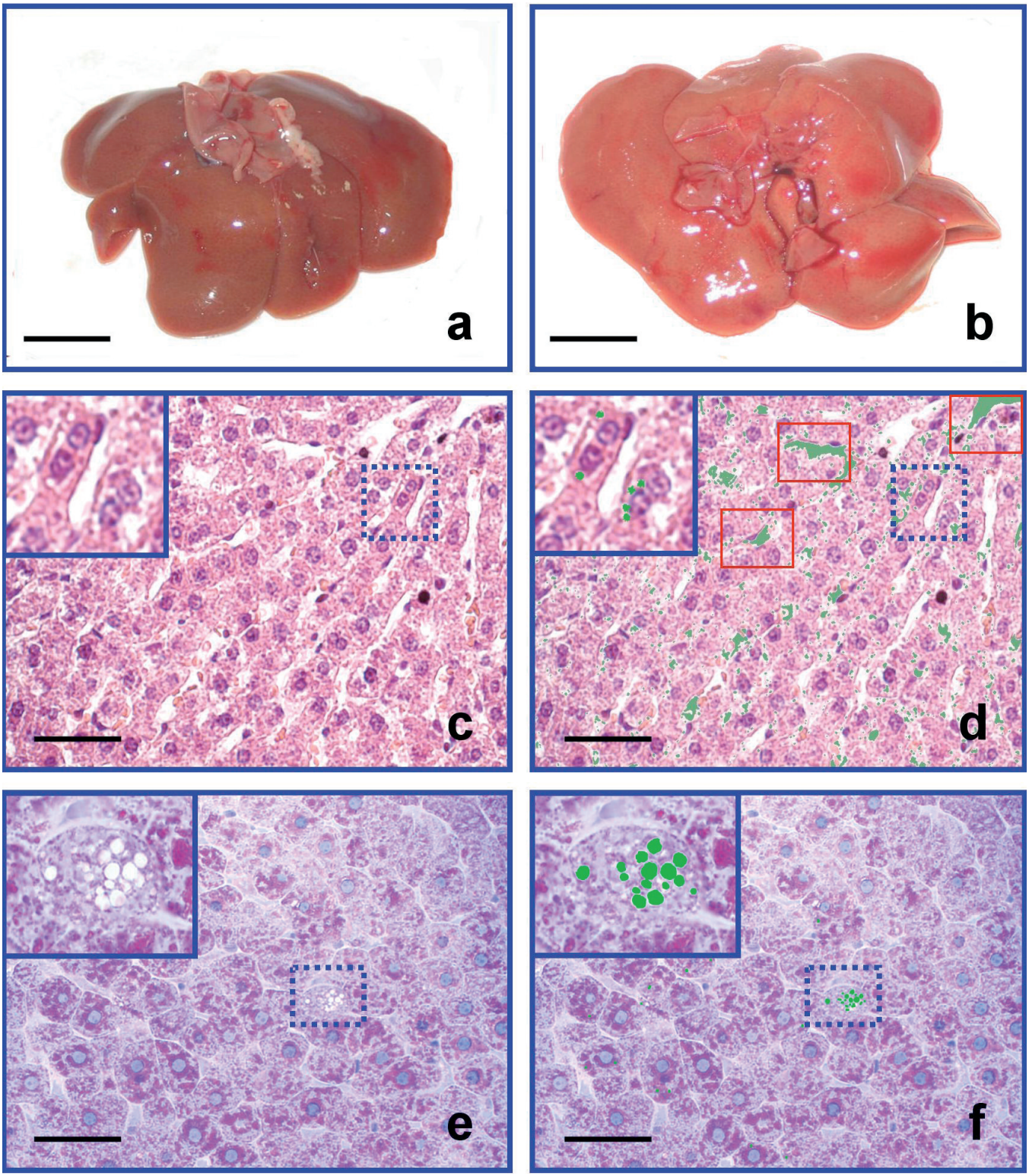

Fig. 2. Gross anatomy of control rat liver **(a)** and liver with steatosis experimentally induced by a 30-day choline deficient diet **(b)**. The fatty liver is clearly increased in mass and has a yellowish appearance. **c-f.** Lipid contents in hepatocytes of control rats. **c, d.** Section of liver samples embedded in paraffin wax stained with H&E, showing rare lipid droplets; insets, magnification of dashed rings. **d.** Selection (green spots) of lipid areas by automated computerised method; red rings, unspecific selection of sinusoids as lipid droplets. **e, f.** Semi-thin section of liver samples embedded in epoxy resin stained with PAS-TB. **f.** Selection (green spots) of lipid areas by automated computerised method. Bars: a, b, 1 cm; c, d, e, f, 90 µm.

was observed in the control counterparts. Steatosis was mostly microvesicular and mostly in the periportal area. Glycogen stores appeared moderately reduced, and sinusoids were scarcely dilated (Fig. 3a). Table 1 shows the percentages of fat content obtained from paraffin and epoxy resin sections, respectively, at 0, 3, 7, 14 and 30 days of diet. Data presented are based on the use of all morphological operators, including the eccentricity filter. Table 2 summarizes the percentages of total lipids measured as microvesicles. When H&E slides prepared from the paraffin-embedded samples were analyzed by a software based only on chromatic-based criteria for lipid selection, unspecific selection of sinusoids as lipid areas was observed (Fig. 3b, red rings). The thickness of the paraffin sections, moreover, caused the overlapping of

Table 1. Automated software analysis of fat content in the liver of rats fed a choline-deficient diet.

Time (days)	Paraffin embedded sections	Epoxy resin embedded sections	p *
0	1.2±0.2	1.4±0.3	0.087 (NS)
3	18.8±1.1	10.8±0.9	<0.01
7	40.3±2.2	24.5±1.8	<0.01
14	44.5±1.7	30.5±2.4	<0.01
30	62.1±2.5	60±1.8	0.052 (NS)

Data, expressed in percentage, are mean±SE; * Student's t -test between each group at each time-point; NS, not significant.

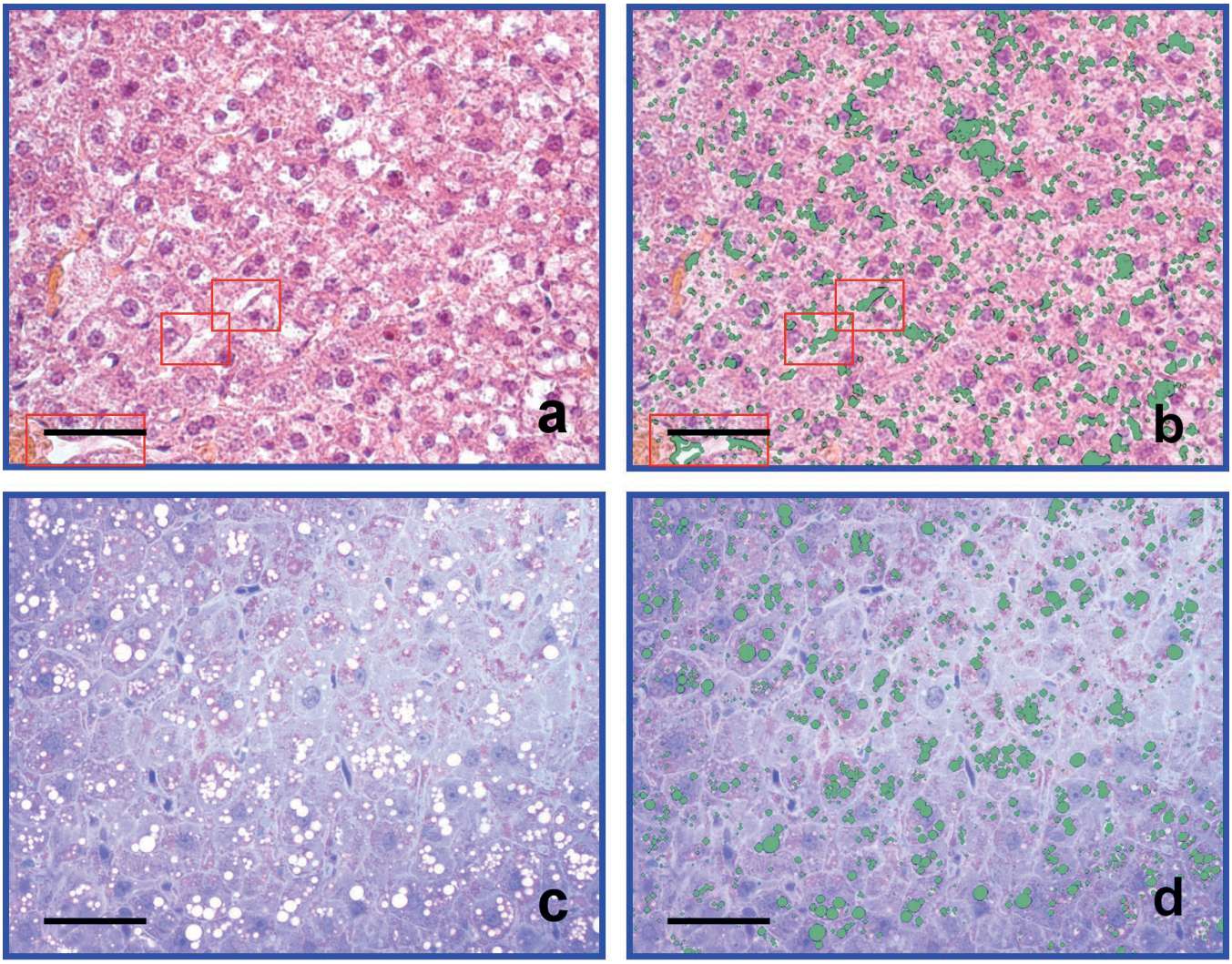

Fig. 3. Fat infiltration in rat liver parenchyma after 3 days of choline-deficient diet. **a, b.** Section of liver samples embedded in paraffin wax stained with H&E. **b.** Selection (green spots) of lipid areas by automated computerised method. Red rings: sinusoids erroneously selected as lipid droplets. **c, d.** Semi-thin section of liver samples embedded in epoxy resin stained with PAS-TB. **d.** Selection (green spots) of lipid areas by automated computerised method. Bars: 90 µm.

individual microvesicles and this was biased since they were computed as macrovesicles. The distribution of macro- and microvesicles was better documented with semi-thin sections obtained from resin-embedded samples (Fig. 3c). Image analysis of paraffin sections showed that the liver parenchymal fat content in choline-deficient fed rats after three days was 18.8±1.1% (70% as microvesicles), whereas the fat content measured with the resin sections was of a lower extent (10.8±0.9%; 93% as microvesicles) (Fig. 3d). At day 7 of the choline-deficient diet, hepatocyte steatosis was still mainly microvesicular. Nevertheless, the number of vesicles was higher than at day 3, leading to the apparent coalescence of microvesicles to form macrovesicles. The cytoplasm was still relatively abundant (Fig. 4a). Automatic

Table 2. Automated software analysis of percent fat microvesicles in the liver of rats fed a choline-deficient diet.

	Percent microvesicles vs. total lipids	
Days	Paraffin embedded sections	Epoxy resin embedded sections
0	98	100
3	70	93
7	30	57
14	15	35
30	5	13

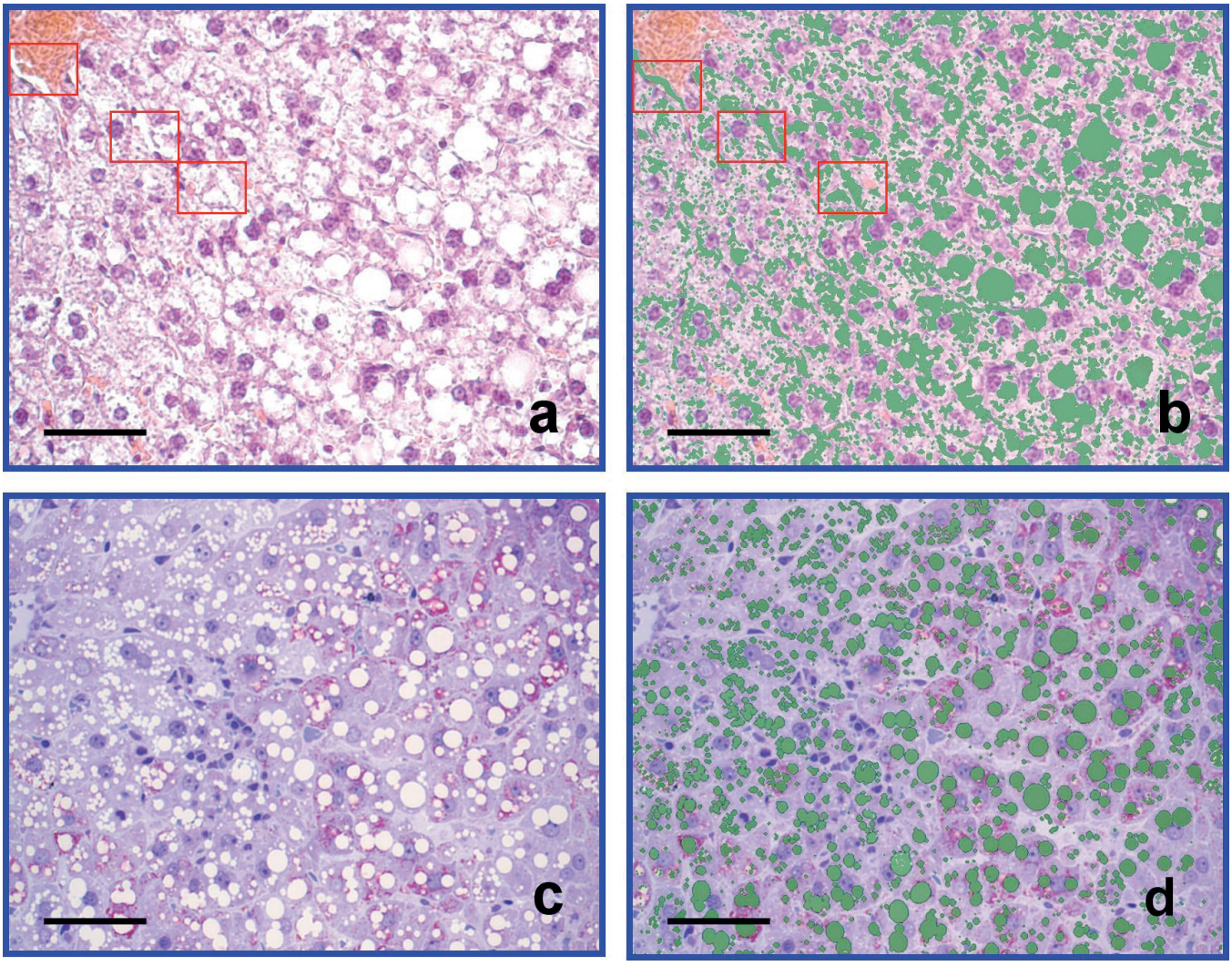

Fig. 4. Fat infiltration in rat liver parenchyma after 7 days of choline-deficient diet. **a, b.** Section of liver samples embedded in paraffin wax stained with H&E. **b.** Selection (green spots) of lipid areas by automated computerised method. Red rings: sinusoids erroneously selected as lipid droplets. **c, d.** Semi-thin section of liver samples embedded in epoxy resin stained with PAS-TB. **d.** Selection (green spots) of lipid areas by automated computerised method. Bars: 90 µm.

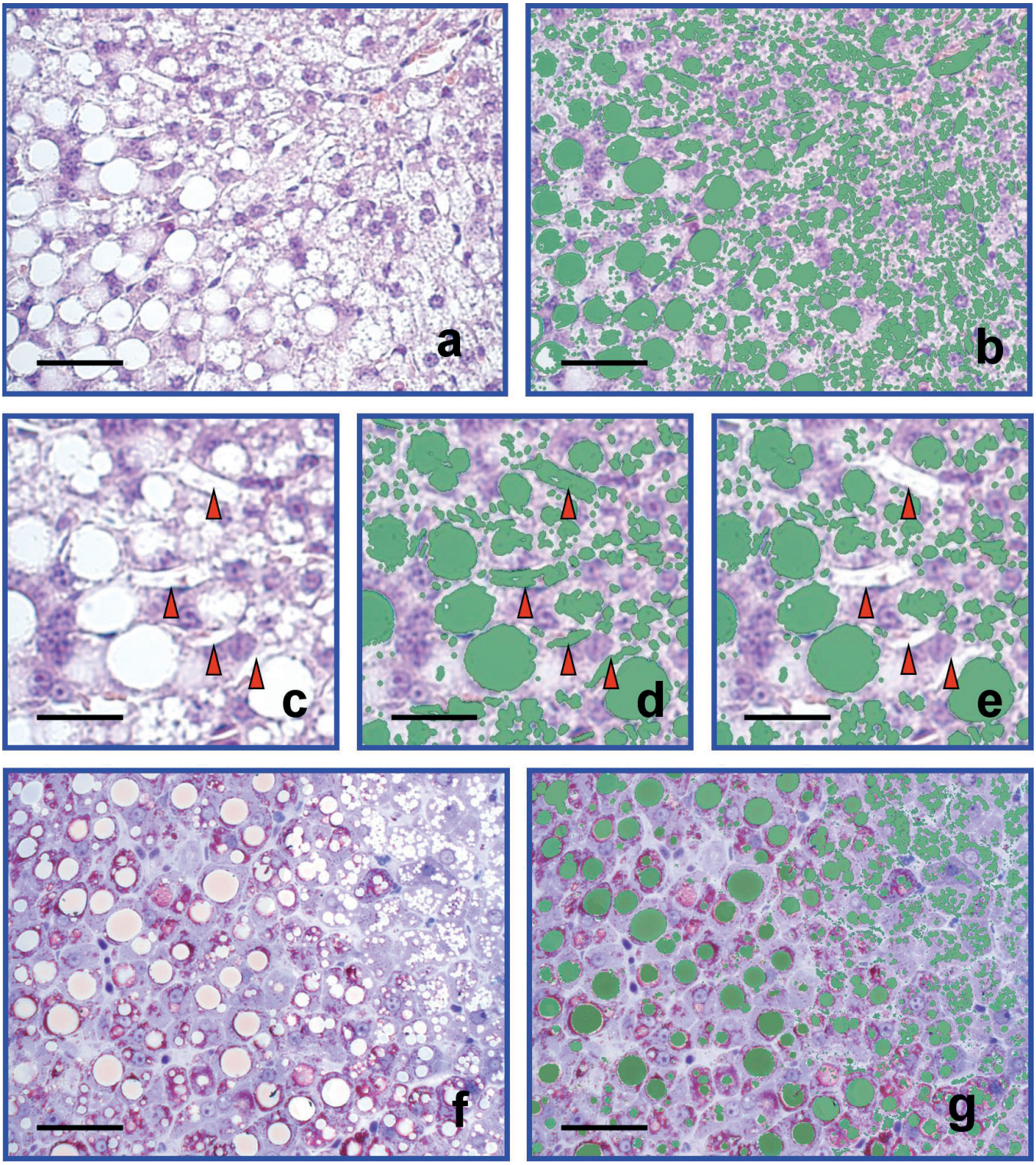

Fig. 5. Fat infiltration in rat liver parenchyma after 14 days of choline-deficient diet. **a-e.** Section of liver samples embedded in paraffin wax stained with H&E. **b.** Selection (green spots) of lipid areas by automated computerised method. **c.** Detail of Fig 3a showing some sinusoids (arrowheads) interposed between adjacent hepatocytes. **d.** Unspecific selection of the same sinusoids as lipid areas (arrowheads) resulting from image analysis performed exclusively with a chromatic filter. **e.** Unspecific selection of the sinusoids (arrowheads) was eliminated by introducing a morphological operator which contemplates the shape factor in addition to the chromatic one for the selection of lipid areas. **f, g.** Semi-thin section of liver samples embedded in epoxy resin stained with PAS-TB. **g.** Selection (green spots) of lipid areas by automated computerised method. Bars: a, b, f, g, 90 µm; c, d, e, 45 µm.

selection of lipid areas based only on chromatic criteria showed notable background, sometimes associated with non-specific sinusoid selection as lipid areas (Fig. 4b). The mean percentage value of fat content obtained from image analysis of paraffin sections (35.4±2.2%; 30% as microvesicles) was significantly higher ($P<0.01$) than in the resin sections (24.5±1.8%, 57% as microvesicles) (Fig. 4c,d). After 14 days of choline-deficient diet, steatosis became a microvesicular-macrovesicular type (Fig. 5a), with a remarkable prevalence of macrovesicles in the periportal area. Unspecific selection of sinusoids was seen with sections analysed solely with a chromatic filter (Fig. 5b-d). The use of a morphological operator for the selection of lipid areas either eliminated, or strongly reduced, both background and unspecific marking of sinusoids (Fig. 5e). Also, at day 14, the fat content measured by image analysis of paraffin sections was 44.5±1.7% (15% of total lipids as microvesicles), significantly higher than the one measured with the resin sections (30.5±2.7%; 35% as microvesicles) (Fig. 5f,g). At 7 and 14 days glycogen stores were of a lesser extent than controls. At day 30, liver steatosis appeared mainly macrovesicular (Fig. 6a). Most hepatocytes contained a single large lipid droplet surrounded by a thin ring of cytoplasm. The nucleus was flattened and displaced peripherally. Glycogen stores were of scarce extent. The fat content of the paraffin sections was of 62.1±2.5% (5% as microvesicles) (Fig. 6b) and consistent with that measured by analyzing the resin sections (60±1.8%; 13% as microvesicles) (Fig. 6c,d). The applicability of

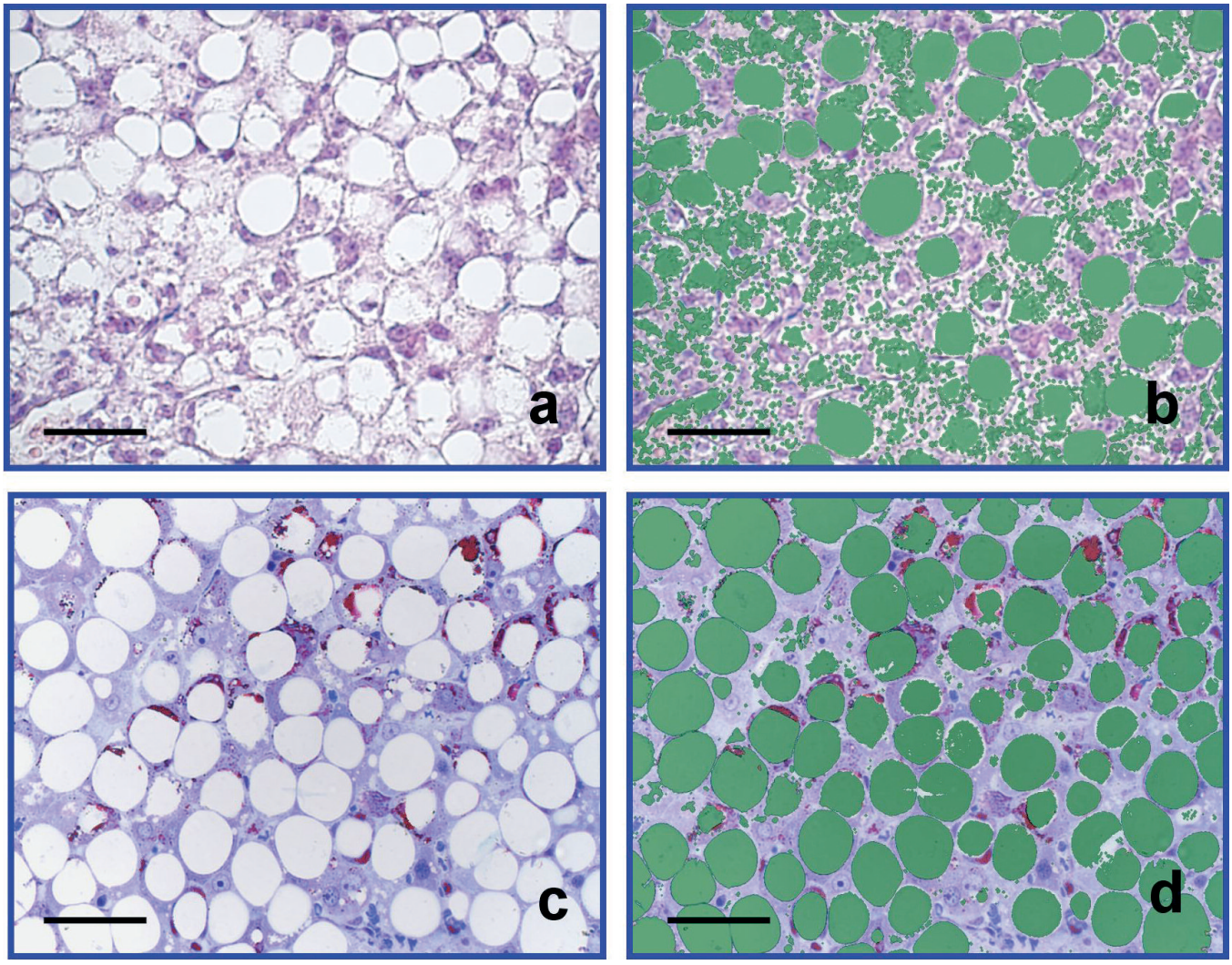

Fig. 6. Fat infiltration in rat liver parenchyma after 30 days of choline-deficient diet. **a, b.** Section of liver samples embedded in paraffin wax stained with H&E. **b.** Selection (green spots) of lipid areas of the same section by automated computerised method. Red rings: unspecific marking of sinusoids. **c, d.** Semi-thin section of liver samples embedded in epoxy resin stained with PAS-TB. **d.** Selection (green spots) of lipid areas by automated computerised method. Bars: 90 µm.

this automated methodology to human fatty liver was verified on specimens obtained from liver biopsy of a morbidly obese patient undergoing bariatric surgery. Remarkable fat infiltration was seen by simple histological analysis (Fig. 7a). Steatosis resulted mainly of macrovesicular type (84.3% of total lipids) (Fig. 7a,d). As with the rat liver sections, unspecific selection of sinusoids was seen with sections analyzed exclusively with a chromatic filter (Fig. 7b). The use of a morphological operator for the selection of lipid areas eliminated the unspecific selection of sinusoids (Fig. 7c). Distribution of macro- and microvesicles was better documented by semi-thin sections obtained from resin embedded samples (Figs. 7d,e). No significant differences were found between the total lipid area obtained by automated image analysis of paraffin sections and the ones obtained from epoxy resin sections (43.56±2.1% and 45.5±1.4%, respectively).

Discussion

Liver steatosis is a major emerging health problem,

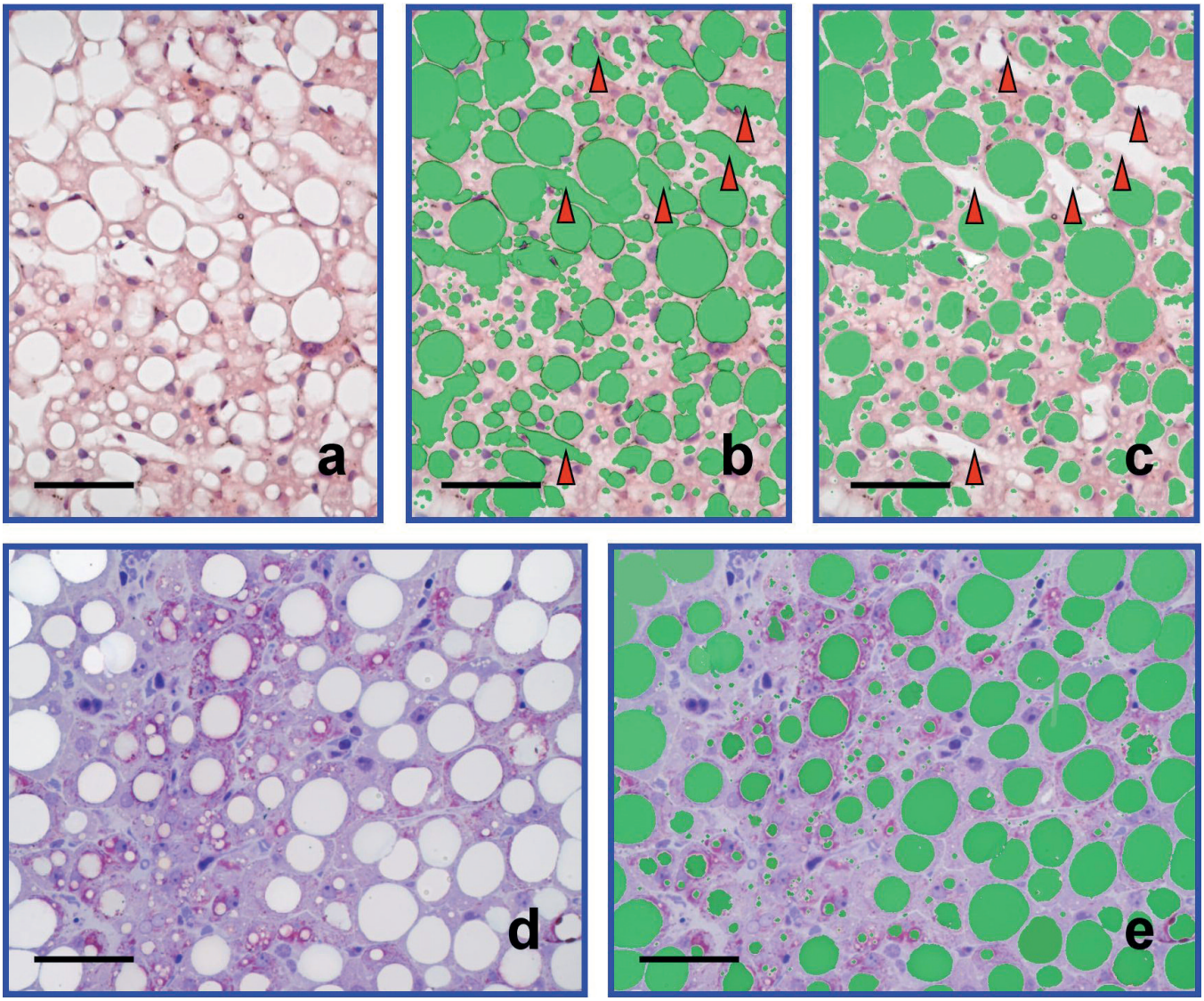

Fig. 7. Morphometric and quantitative analysis of fat infiltration in human steatotic liver. **a-c.** Section of liver samples embedded in paraffin wax stained with H&E. **b.** Selection (green spots) of lipid areas by automated computerised method. Note the unspecific selection of some sinusoids as lipid areas resulting from image analysis performed exclusively with a chromatic filter (arrowheads). **c.** Unspecific marking of the sinusoids (arrowheads) was eliminated by introducing a morphological operator which contemplates the shape factor in addition to a chromatic one for counting lipid droplets. **d, e.** Semi-thin section of liver samples embedded in epoxy resin stained with PAS-TB. **e.** Selection (green spots) of lipid areas by automated computerised method. Bars: 90 µm.

often associated with metabolic disorders, alcoholic liver disease, and chronic viral hepatitis (Calamita and Portincasa, 2007). Even a simple fatty liver may have an unfavorable clinical outcome, with potential evolution toward cirrhosis and hepatocellular carcinoma, as in the case of the NAFLD/NASH sequence (Saito et al., 2007). Thus, accurate morphometric and quantitative evaluation of the degree of steatosis, together with a number of other features, including necroinflammatory and fibrotic changes, plays a key role when assessing the fatty liver (Brunt et al., 1999; Matteoni et al., 1999; Kleiner et al., 2005; Saito et al., 2007). As reported for NASH, however, sampling error of liver biopsy can result in substantial misdiagnosis and staging inaccuracies (Ratziu et al., 2005; Merriman et al., 2006). We used a choline-deficient diet (Grattagliano et al., 2000, 2003) that reliably induces fatty liver in rodents due to triglyceride accumulation, which is not associated with weight loss or significant steatohepatitis (Kulinski et al., 2004). Observations on fatty liver changes were also extended to human liver. The degree of lipid infiltration in liver disease is commonly assessed on histological sections by semi-quantitative scoring systems (Nagore and Scheuer, 1988). Recently, automated computerized methods have been also introduced (Auger et al., 1986; Zaitoun et al., 2001; Marsman et al., 2004), having recourse to liver embedded paraffin sections stained with H&E and, for the image analysis, to commonly available commercial software. Since the results of image analysis are highly dependent on the quality of the histological specimens, we aimed to markedly improve the currently available automated computerized methods by (i) using semi-thin histological sections (2 μm) obtained from epoxy resin embedded samples, (ii) staining the sections with PAS-TB to label all cytoplasm areas not occupied by lipid droplets and (iii) using a specific software supplied with a morphological operator in addition to a chromatic one to select lipid droplets. This approach has the advantage of providing well defined histological images, with better delimitation of microvesicles, even when small in size. Also, any errors that may occur when the automated lipid selection is based only on chromatic criteria are avoided, because the program considers both shape and color as factors for selecting the areas of lipid infiltration. To check the validity of our method, the automated evaluation of paraffin-embedded sections was compared with that using the epoxy resin sections in a well validated rodent model of fatty liver. The choline-deficient diet induced steatotic changes starting in the periportal zone, as previously described (Rushmore et al., 1987; Nieto and Rojkind, 2007). During the 30 days of diet, we observed a full range of steatotic changes: microvesicular (early stage), micro- and macrovesicular (intermediate stage) and mainly macrovesicular (late stage at 30 days of diet).

However, we noticed that underestimation of lipid microvesicles occurs when steatotic livers are analyzed as paraffin-embedded sections. This is an exceedingly important aspect when evaluating the clinical and prognostic profile of patients with liver diseases. Of note, lipid underestimation is strongly reduced when livers are embedded in epoxy resin (Table 2). When comparing the percentages of lipid microvesicles and macrovesicles in rat steatotic livers, the greatest difference is observed at the microvesicular stage (day 3 in our experimental model), a critical time in the pathogenesis of steatosis. Another critical parameter in analyzing liver steatosis regards the operator used to select the areas of lipid infiltration within hepatic parenchyma. In paraffin sections stained with H&E, the degree of steatosis appears to be overestimated when using only the chromatic operator as a criterion for selecting the areas of lipid accumulation. This is likely due to the fact that the automatic selection includes non-lipid areas with the same histological colour as the lipid areas. False positive areas may relate to sinusoidal spaces or glycogen stores and REL areas within hepatocyte. These drawbacks are considerably reduced by using semi-thin sections stained with PAS-TB, where the definition of the lipid droplets is of a satisfactory level for a careful chromatic distinction between true and some of the false positive areas of lipid infiltration. Besides, background or unspecific selection of sinusoids was drastically reduced with our image analysis software when working with a morphological operator in addition to a chromatic one. This sophistication led to the exclusion of false positive areas with the same colour as the lipid droplets but of irregular shape (circular or ovoid areas were considered as true lipid ones). The macrovesicles-to-microvesicles ratio produces overestimates when the intermediate stage (micro- and macrovesicular stage) is analysed using paraffin sections. Indeed, due to the thickness of the sections, overlapping microvesicles are read as macrovesicles by the computerized system. Overestimation of this ratio is a recurrent (and still unsolved) problem threatening liver pathologists, as demonstrated by a previous comparative study of automated image analysis and semi-quantitative estimations of alcoholic liver steatosis (Auger et al., 1986).

At the macrovesicular stage of steatosis (day 30 in our rat model) no significant differences are found between data obtained from paraffin and epoxy resin sections. This is reasonably explained by the fact that at such an advanced stage of steatosis microvesicles coalesce, forming single (or few) lipid droplets occupying most of the cytoplasm, a situation that is correctly counted by the image analysis software. Moreover, background is scarce and errors due to unspecific staining of sinusoids are of negligible extent since their lumen is reduced due to the dilation to which hepatocytes undergo in steatosis (Rao et al., 2001). An important issue in this work is that the automated computerized methods may be usefully employed in the morphometric and quantitative estimation of fat infiltration in samples of human liver biopsies or surgery resections. In conclusion, our automated image analysis technique applied to semi-thin sections prepared from

liver samples embedded in epoxy resin and stained with PAS-TB considerably improves the topographic, morphometric and quantitative evaluation of liver steatosis. This becomes particularly valuable when fat infiltration is of microvesicular type, which is generally a more severe disease than the macrovesicular form. Microvesicular steatosis of the liver, has been described in association with a number of clinical features, including acute fatty liver of pregnancy, congenital defects of fatty acid beta oxidation, Reye's syndrome, toxicity of several drugs, defects of urea cycle enzymes, cholesterol ester storage disease (Hautekeete et al., 1990).

Of note, the procedure seems to have the requisites to be applied to human liver samples, offering promising diagnostic and prognostic perspectives.

References

Armitage P. and Berry G. (1994). Statistical methods in medical research. Blackwell Science Ltd. Oxford.

Auger J., Schoevaert D. and Martin E.D. (1986). Comparative study of automated morphometric and semiquantitative estimations of alcoholic liver steatosis. Anal. Quant. Cytol. Histol. 8, 56-62.

Brunt E.M., Janney C.G., Di Bisceglie A.M., Neuschwander-Tetri B.A. and Bacon B.R. (1999). Nonalcoholic steatohepatitis: a proposal for grading and staging the histological lesions. Am. J. Gastroenterology 94, 2467-2474.

Burt A.D., Mutton A. and Day C.P. (1998). Diagnosis and interpretation of steatosis and steatohepatitis. Semin. Diagn. Pathol. 15, 246-258.

Calamita G. and Portincasa P. (2007). Present and future therapeutic strategies in non-alcoholic fatty liver disease. Export. Opin. Ther. Targets 11, 1231-1249.

Dawson B. and Trapp R. G. (2001). Basic & Clinical Biostatistics. McGraw-Hill. New York.

Fong D.G., Nehra V., Lindor K.D. and Buchman A.L. (2000). Metabolic and nutritional considerations in nonalcoholic fatty liver. Hepatology 32, 3-10.

Grattagliano I., Caraceni P., Portincasa P., Domenicali M., Palmieri V.O., Trevisani F., Bernardi M. and Palasciano G. (2003). Adaptation of subcellular glutathione detoxification system to stress conditions in choline-deficient diet induced rat fatty liver. Cell. Biol. Toxicol. 19, 355-366.

Grattagliano I., Vendemiale G., Caraceni P., Domenicali M., Nardo B., Cavallari A., Trevisani F., Bernardi M. and Altomare E.. (2000). Starvation impairs antioxidant defense in fatty livers of rats fed a choline-deficient diet. J. Nutr. 130, 2131-2136.

Haralick R.M. and Shapiro L. G. (1992). Computer and Robot Vision. Addison-Wesley. New York. pp. 158-205.

Hautekeete M.L., Degott C. and Benhamou J.P. (1990). Microvesicular steatosis of the liver. Acta Clin. Belg. 45, 311-26.

Kahn R., Buse J., Ferrannini E. and Stern M. (2005). The metabolic syndrome: time for a critical appraisal. Joint statement from the American Diabetes Association and the European Association for the Study of Diabetes. Diabetologia 48, 1684-1699.

Kleiner D.E., Brunt E.M., Van Natta M., Behling C., Contos M.J., Cummings O.W., Ferrell L.D., Liu Y.C., Torbenson M.S., Unalp-Arida A., Yeh M., McCullough A.J. and Sanyal A.J. (2005). Design and validation of a histological scoring system for nonalcoholic fatty liver disease. Hepatology 41, 1313-1321.

Kulinski A., Vance D.E. and Vance J.E. (2004). A choline-deficient diet in mice inhibits neither the CDP-choline pathway for phosphatidylcholine synthesis in hepatocytes nor apolipoprotein B secretion. J. Biol. Chem. 279, 23916-23924.

Loguercio C., De Girolamo V., De Sio I., Tuccillo C., Ascione A., Baldi F., Budillon G., Cimino L., Di Carlo A., Di Marino M.P., Morisco F., Picciotto F., Terracciano L., Vecchione R., Verde V. and Del Vecchio B.C. (2001). Non-alcoholic fatty liver disease in an area of southern Italy: main clinical, histological, and pathophysiological aspects. J. Hepatol. 35, 568-574.

Loguercio C., De Simone T., D'Auria M.V., De Sio I, Federico A., Tuccillo C., Abbatecola A.M., Del Vecchio B.C. and the AISF Group. (2004). Non-alcoholic fatty liver disease: a multicentre clinical study by the Italian Association for the Study of the Liver. Dig. Liver Dis. 36, 398-405.

Ludwig J., Viggiano T.R., McGill D.B. and Oh B.J. (1980). Nonalcoholic steatohepatitis: Mayo Clinic experiences with a hitherto unnamed disease. Mayo Clin. Proc. 55, 434-438.

Marchesini G., Bugianesi E., Forlani G., Cerrelli F., Lenzi M., Manini R., Natale S., Vanni E., Villanova N., Melchionda N. and Pizzetto M. (2003). Nonalcoholic fatty liver, steatohepatitis, and the metabolic syndrome. Hepatology 37, 917-923.

Marsman H., Matsushita T., Dierkhising R., Kremers W., Rosen C., Burgart L. and Nyberg S.L. (2004). Assessment of donor liver steatosis: pathologist or automated software? Hum. Pathol. 35, 430-435.

Matteoni C.A., Younossi Z.M., Gramlich T., Boparai N., Liu Y.C. and McCullough A.J. (1999). Nonalcoholic fatty liver disease: a spectrum of clinical and pathological severity. Gastroenterology 116, 1413-1419.

Merriman R.B., Ferrell L.D., Patti M.G., Weston S.R., Pabst M.S., Aouizerat B.E. and Bass N.M. (2006). Correlation of paired liver biopsies in morbidly obese patients with suspected nonalcoholic fatty liver disease. Hepatology 44, 874-880.

Nagore N. and Scheuer P.J. (1988). The pathology of diabetic hepatitis. J. Pathol. 156, 155-160.

Neuschwander-Tetri B.A. and Bacon B.R. (1996). Nonalcoholic steatohepatitis. Med. Clin. North Am. 80, 1147-1166.

Nieto N. and Rojkind M. (2007). Repeated whiskey binges promote liver injury in rats fed a choline-deficient diet. J. Hepatol. 46, 330-339.

Poonawala A., Nair S.P. and Thuluvath P.J. (2000). Prevalence of obesity and diabetes in patients with cryptogenic cirrhosis: a case-control study. Hepatology 32, 689-692.

Portincasa P., Grattagliano I., Palmieri V.O. and Palasciano G. (2006). Current pharmacological treatment of nonalcoholic fatty liver. Curr. Med. Chem. 13, 2889-2900.

Portincasa P., Grattagliano I., Palmieri V.O. and Palasciano G. (2005). Nonalcoholic steatohepatitis: recent advances from experimental models to clinical management. Clin. Biochem. 38, 203-217.

Rao M.S., Papreddy K., Abecassis M. and Hashimoto T. (2001). Regeneration of liver with marked fatty change following partial hepatectomy in rats. Dig. Dis. Sci. 46,1821-1826.

Ratziu V., Charlotte F., Heurtier A., Gombert S., Giral P., Bruckert E., Grimaldi A., Capron F. and Poynard T. (2005). Sampling variability of liver biopsy in nonalcoholic fatty liver disease. Gastroenterology 128, 1898-1906.

Raubenheimer P.J., Nyirenda M.J. and Walker B.R. (2006). A choline-

deficient diet exacerbates fatty liver but attenuates insulin resistance and glucose intolerance in mice fed a high-fat diet. Diabetes 55, 2015-2020.

Reddy J.K. and Mannaerts G.P. (1994). Peroxisomal lipid metabolism. Annu. Rev. Nutr. 14, 343-370.

Rushmore T.H., Ghazarian D.M., Subrahmanyan V., Farber E. and Ghoshal A.K. (1987). Probable free radical effects on rat liver nuclei during early hepatocarcinogenesis with a choline-devoid low methionine diet. Cancer Res. 47, 6731-6740.

Saito T., Misawa K. and Kawata S. (2007). 1. Fatty liver and non-alcoholic steatohepatitis. Intern. Med. 46, 101-103.

Sherlock S. (1995). Alcoholic liver disease. Lancet 345, 227-229.

Urena M.A., Ruiz-Delgado F.C., Gonzalez E.M., Segurola C.L., Romero C.J., Garcia I.G., Gonzalez-Pinto I. and Gomez S.R. (1998). Assessing risk of the use of livers with macro and microsteatosis in a liver transplant program. Transplant Proc. 30, 3288-3291.

Van den Boomgard R. and van Balen R. (1992). Methods for fast morphological image transforms using bitmapped images. Computer Vision, Graphics, and Image Processing: Graphical Models and Image Processing 54: 252-254.

Zaitoun A.M., Al M.H., Awad S., Ukabam S., Makadisi S. and Record C.O. (2001). Quantitative assessment of fibrosis and steatosis in liver biopsies from patients with chronic hepatitis C. J. Clin. Pathol. 54, 461-465.

Accepted July 25, 2008